Field-induced spin-density-wave and butterfly spectrum in three dimensions

M. Koshino and H. Aoki
Department of Physics, University of Tokyo, Hongo, Tokyo 113-0033, Japan

T. Osada
Institute for Solid State Physics, University of Tokyo, Kashiwa, Chiba 277-8581, Japan
(Received 12 December 2001; published 29 April 2002)

Landau's quantization for incompletely nested Fermi surfaces is known to give rise to magnetic-field-induced spin-density waves (FISDW's) in two-dimensional organic metals. Here we show that three-dimensional (3D) systems can have 3D-specific series of FISDW phases as energetically stable states, for which we clarify how and why they appear as the magnetic field is tilted. Each phase is characterized by a quantized Hall effect for each σ_{xy} and σ_{zx} that reside on a fractal-like Hofstadter's butterfly.

DOI: 10.1103/PhysRevB.65.205311 PACS number(s): 72.15.Gd, 75.30.Fv, 74.70.Kn

I. INTRODUCTION

Rich electronic states arising from the nesting of Fermi surfaces continue to provide fascination in various classes of materials. Organic crystals provide particularly versatile Fermi surfaces, and it has indeed been shown[1] that a curious series of spin-density-wave (SDW) states emerge in strong magnetic fields in a family of quasi-two-dimensional organic conductors $(\mathrm{TMTSF})_2X$ (TMTSF is tetramethyltetraselenafulvalene and $X=\mathrm{PF}_6$, etc.), called the Bechgaard salt. The field-induced spin-density wave (FISDW) occurs when the nesting of the Fermi surface is incomplete. The Landau quantization in the pockets formed as a result of an incompletely nesting then causes a series of gaps to appear around the main SDW gap.[2,3] Since E_F always lies in the largest Landau gap, an integer quantum Hall effect arises. When the magnetic field is increased, successive phase transitions take place because the energetically favorable SDW nesting vector jumps along the way, which results in discontinuous changes of the Hall conductivity. This has been considered for the TMTSF compound[4] that happens to have very anisotropic transfer energies between molecules with $t_x:t_y:t_z \sim 1:0.1:0.003$, so that the system is almost perfectly two dimensional (2D).

So the challenging problem we address here is as follows: (i) can we have such Landau-quantization-assisted FISDW states in three-dimensional systems, not as a remnant of the 2D FISDW but as 3D-specific, energetically favorable states, and if so, (ii) how and why do the successive phase transitions arise in three dimensions? Lebed[5] introduced third direction hopping to a FISDW, and several authors[6,8,9] studied the quantum Hall effect in a 3D FISDW, where Hall conductivities σ_{xy} and σ_{zx} are predicted to be quantized, respectively. However, the condition for the emergence of 3D FISDW phase itself has not been worked out except for a limited case for $(\mathrm{TMTSF})_2X$ where three dimensionality is very small.[8] So it has remained to be clarified whether and how FISDW phases really do exist in three dimensions.

This is exactly the purpose of the present paper. We consider the possibility of FISDW phases in 3D systems in magnetic fields, where we shall show that the favorable situation is anisotropic 3D systems with an anisotropy such that the transfer energies satisfy $t_x \gg t_y \sim t_z$ [as contracted with $t_x \gg t_y \gg t_z$ in $(\mathrm{TMTSF})_2X$]. With a varied magnitude and orientation of the magnetic field $\boldsymbol{B}=(0,B_y,B_z)$, we have optimized the SDW nesting vector to show that a series of 3D FISDW phases do indeed exist, which is best expressed as a phase diagram against (B_y,B_z). The phases comprise rich families, where they are characterized by quantized Hall conductivities σ_{xy} and σ_{zx} as one hallmark of the 3D nature. On the energy axis, the FISDW is seen to reside on a fractal energy spectrum like Hofstadter's butterfly,[10] which, curiously, also indicates the 3D-specific nature of the 3D FISDW. In fact this can be regarded as one realization, through a density-wave formation, of the butterfly and the quantum Hall effect in three dimensions we have proposed on a general mathematical basis.[11] An intuitive reason why the butterfly spectrum arise in the 3D FISDW is discussed in terms of the topology of the incompletely nested Fermi surface in three dimensions in Sec. V.

II. FORMULATION FOR THE 3D FISDW

We consider a simple orthorhombic metal with an energy dispersion

$$\epsilon(\boldsymbol{k}) = -t_x \cos k_x a - t_y \cos k_y b - t_z \cos k_z c, \tag{1}$$

where a,b, and c are lattice constants and the transfer energies are assumed to satisfy $t_x \gg t_y, t_z$ (i.e., are quasi-1D). The dispersion along k_x around the Fermi energy can be approximated as a linear function $v_F(|k_x|-k_F)$ [with $\hbar=1$ and $\epsilon(\boldsymbol{k})$ measured from E_F], while the three dimensionality (warping of the Fermi surface) can be described by the expansion in t_y and t_z as

$$\epsilon(\boldsymbol{k}) = v_F(|k_x|-k_F) + \epsilon_\perp(\boldsymbol{k}_\perp), \tag{2}$$

$$\begin{aligned}\epsilon_\perp(\boldsymbol{k}_\perp) = &-t_y \cos k_y b - t_z \cos k_z c - t_y' \cos 2k_y b - t_z' \cos 2k_z c\\ &- t_{yz}'[\cos(k_y b + k_z c) + \cos(k_y b - k_z c)],\end{aligned} \tag{3}$$

where $\boldsymbol{k}_\perp \equiv (k_y, k_z)$, and

$$t'_y=\alpha t_y^2/t_x,$$

$$t'_z=\alpha t_z^2/t_x, t'_{yz}=2\alpha t_y t_z/t_x, \tag{4}$$

with $\alpha=-(\cos k_F a)/(4\sin^2 k_F a)$.

Let us apply a magnetic field $(0,B_y,B_z)$ normal to the conductive axis x. We take the spin quantization axis parallel to z. We assume that a SDW is the most likely instability as in the Bechgaard salts,[7] and look at the mean-field equation for the wave function with the 3D nesting vector $\boldsymbol{q}=(q_x,q_y,q_z)$, which can be written[2,3]

$$\begin{pmatrix} E-H_\uparrow(x) & \Delta(x) \\ \Delta^*(x) & E-H_\downarrow(x)\end{pmatrix}\begin{pmatrix} u(x) \\ v(x)\end{pmatrix}=0,$$

$$H_\uparrow(x)=-iv_F\partial_x+\boldsymbol{\epsilon}_\perp(\boldsymbol{k}_\perp-e\boldsymbol{A}_\perp),$$

$$H_\downarrow(x)=+iv_F\partial_x+\boldsymbol{\epsilon}_\perp(\boldsymbol{k}_\perp-\boldsymbol{q}_\perp-e\boldsymbol{A}_\perp), \tag{5}$$

where $\boldsymbol{A}_\perp=(B_z x,-B_y x)$ is the vector potential, and the band energy measured from $-v_F k_F$. $H_\uparrow(H_\downarrow)$ is the Hamiltonian for an electron on the right Fermi surface with up-spin (or on the left Fermi surface with down-spin), while $u(v)$ is the corresponding wave function for an up-spin electron on the right Fermi surface (down-spin on the left). $\Delta(x)$ represents the mean-field electron interaction, which can be approximately written as a single-mode function $\Delta(x)\sim\Delta e^{iq_x x}$. We determine Δ and $\boldsymbol{q}$ self-consistently so as to minimize the free energy at $T=0$ (i.e., the ground-state energy). The SDW also mixes down-spin states around the right Fermi surface and up-spins around left Fermi surface, which defines another order parameter. The phase difference between the two order parameters specifies the spin order direction on the xy plane.

If we separate out the $\boldsymbol{\epsilon}_\perp$-dependent phase as

$$u(x)=\tilde{u}(x)\exp\left[-\frac{i}{v_F}\int_0^x \boldsymbol{\epsilon}_\perp(\boldsymbol{k}_\perp-e\boldsymbol{A}_\perp)dx'\right],$$

$$v(x)=\tilde{v}(x)\exp\left[+\frac{i}{v_F}\int_0^x \boldsymbol{\epsilon}_\perp(\boldsymbol{k}_\perp-\boldsymbol{q}_\perp-e\boldsymbol{A}_\perp)dx'\right],$$

$$\Delta(x)=\tilde{\Delta}(x)\exp\left(-\frac{i}{v_F}\int_0^x[\boldsymbol{\epsilon}_\perp(\boldsymbol{k}_\perp-e\boldsymbol{A}_\perp) + \boldsymbol{\epsilon}_\perp(\boldsymbol{k}_\perp-\boldsymbol{q}_\perp-e\boldsymbol{A}_\perp)]dx'\right). \tag{6}$$

Equation (5) reads

$$\begin{pmatrix} E+iv_F\partial_x & \tilde{\Delta}(x) \\ \tilde{\Delta}^*(x) & E-iv_F\partial_x\end{pmatrix}\begin{pmatrix} \tilde{u}(x) \\ \tilde{v}(x)\end{pmatrix}=0, \tag{7}$$

where the effect of the magnetic field is included in the off-diagonal part, $\tilde{\Delta}$. When we plug Eq. (3) into $\tilde{\Delta}$, we obtain

$$\tilde{\Delta}(x)=\Delta e^{iq_x x}\sum_{n_1\ldots n_6} J_{n_1}(z_1)J_{n_2}(z_2)\times\ldots\times J_{n_6}(z_6) \times e^{-i(n_1+2n_3+n_5+n_6)G_b x-i(n_2+2n_4+n_5-n_6)G_c x+i\delta}, \tag{8}$$

with

$$z_1=2t_y/(G_b v_F)\cos(q_y/2),\quad z_2=2t_z/(G_c v_F)\cos(q_z/2),$$

$$z_3=t'_y/(G_b v_F)\cos q_y,\quad z_4=t'_z/(G_c v_F)\cos q_z,$$

$$z_5=t'_{yz}/[(G_b+G_c)v_F]\cos[(q_y+q_z)/2],$$

$$z_6=t'_{yz}/[(G_b-G_c)v_F]\cos[(q_y-q_z)/2], \tag{9}$$

where J_n is the Bessel function,

$$G_b=eB_z b, G_c=eB_y c,$$

and $\delta(q_y,q_z)$ is a phase factor independent of x. The summation in Eq. (8) can be rearranged into

$$\tilde{\Delta}(x)=\Delta\sum_{mn} I_{mn}e^{i(q_x-mG_b-nG_c)x+i\delta}, \tag{10}$$

where I_{mn} is a summation of products of J_n's. We can see that the energy gaps of width $|\Delta I_{mn}|$ open at $k_x=\pm\frac{1}{2}(q_x-mG_b-nG_c)$. Since the Fermi energy (at $k_x=\pm k_F$) must lie in the largest gap to minimize the energy, we obtain

$$\tfrac{1}{2}(q_x-MG_b-NG_c)=k_F, \tag{11}$$

where M and N are the m and n that give the largest I_{mn}. Thus the x component of the SDW nesting vector becomes $q_x=2k_F+MG_b+NG_c$.[5] Here we assume $k_F\gg G_b,G_c$, which is reasonable as long as typically $B<10^4$ T.

To be precise, gaps other than the one at E_F can affect the stability of the FISDW, but in the weak-coupling regime at $T=0$ we can show that the stability of the FISDW phase is determined by the width of the gap in which E_F resides as shown below. Suppose G_b/G_c is rational with

$$G_b=pG,\quad G_c=qG,$$

where p and q are mutually prime integers. Equation (10) can then be rewritten as

$$\tilde{\Delta}(x)=\Delta\sum_l I_l e^{i(q_x-lG)x+i\delta}, \tag{12}$$

where I_l is the summation of I_{mn} over those (m,n) satisfying $mp+nq=l$. The energy spectrum has a gap at $k_x=\pm\frac{1}{2}(q_x-lG)$ for each integer l. We consider a situation where the gap widths are smaller than the gap intervals. We can then express the energy dispersion along x in the extended zone (shown in Fig. 1) as

$$E^\pm(k_x)=\xi^\pm+\sum_l\left[\mathrm{sgn}(\xi^\pm-l\varepsilon)\sqrt{(\xi^\pm-l\varepsilon)^2+|\Delta I_l|^2}-(\xi^\pm-l\varepsilon)\right], \tag{13}$$

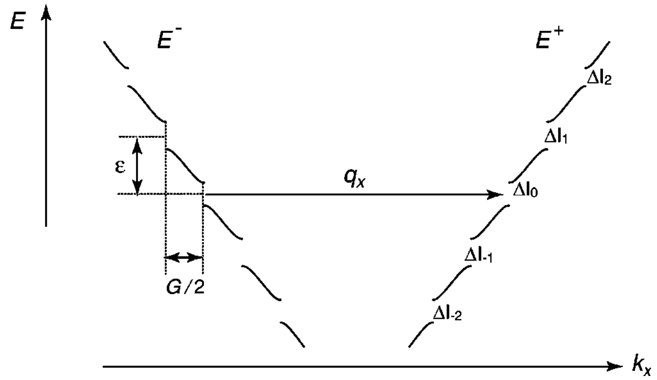

FIG. 1. The structure of the energy spectrum representing Eq. (13) in the text.

where $\xi^{\pm}(k_x)=\pm\hbar v_F(k_x\mp\frac{1}{2}q_x)$ are the dispersions for $\Delta=0$ measured from the gap at $l=0$ for the right (ξ^+) and left (ξ^-) Fermi surfaces with $\varepsilon=\hbar v_F G/2$. The energy gained by opening the gap in the metallic state is

$$F=\frac{|\Delta|^2}{v_0}+\sum_{\boldsymbol{k},\pm}[E^{\pm}(k_x)-\xi^{\pm}(k_x)]. \tag{14}$$

Here $v_0(>0)$ is a molecular-field constant, and the summation taken over $E_F-\xi_c<E^{\pm}(k_x)<E_F$, where ξ_c is a cutoff. If we insert Eq. (13) into this equation, we have

$$F=\frac{|\Delta|^2}{v_0}-D_0\frac{|\Delta I_L|^2}{2}\left(1+\log\frac{4\xi_c^2}{|\Delta I_L|^2}\right)$$
$$+D_0\sum_{l\neq 0}|\Delta I_{L+l}|^2\log\left|\frac{l\varepsilon}{\xi_c+l\varepsilon}\right|, \tag{15}$$

where L is the index of the gap that contains E_F, and D_0 is the density of states for $\Delta=0$ which is assumed to be a constant. From the gap equation, $\partial F/\partial|\Delta|^2=0$, we obtain

$$|\Delta I_L|=2\xi_c\exp\left(\frac{-1}{|I_L|^2 v_0 D_0}+\sum_{l\neq 0}\left|\frac{I_{L+l}}{I_L}\right|^2\log\left|\frac{l\varepsilon}{\xi_c+l\varepsilon}\right|\right), \tag{16}$$

$$F=-D_0\frac{|\Delta I_L|^2}{2}. \tag{17}$$

Thus Δ in general depends not only on the width of the gap at E_F ($\propto I_L$) but also those of other gaps. In the weak-coupling limit $v_0\to 0$, however, Δ is mainly determined by the factor $\exp[-1/(|I_L|^2 v_0 D_0)]$. So larger I_L gives larger Δ in Eq. (16), which gives smaller F in Eq. (17). Therefore, we only have to maximize I in order to minimize the free energy.

III. PHASE DIAGRAM AND HALL CONDUCTIVITY

We have obtained the phase diagram against (B_y,B_z) by maximizing $I_{mn}(q_y,q_z)$ for mesh points on (B_y,B_z) and (q_y,q_z) around (π,π). Figure 2 shows the result for $t_y=t_z$ (a) and $t_y>t_z$ (b). In both cases we do have a series of phases that are characterized by (M,N) defined in Eq. (11). An essential finding here is that there are FISDW phases *specific to three dimensions*, which exist only when both t_y and t_z are nonzero. We can see this by comparing Figs. 2(a) and 2(b), where the 3D-specific phases (shaded) are seen to shrink as $t_z/t_y\to 0$. The 3D-specific phases are classified into several families: $(M,N)=(N,-N)$ phases lying along $\theta\equiv\tan^{-1}(B_y/B_z)=45°$, and $(-2N,0)$ phases around $(B_y,B_z)\simeq(0.1,0)$, etc., and their mirror images $(B_y\leftrightarrow B_z)$. Sun and Maki[8] have shown that a small t_z in $(TMTSF)_2X$ (where $t_z'\propto t_z^2$ neglected) can give rise to a phase with nonzero M and N just at a particular angle of $\boldsymbol{B}$ (Lebed's angle, corresponding to 45° in our model for $b=c$). The Sun-Maki phase is possibly related to the present 3D phases, although it does not belong to the $(N,-N)$ family here.

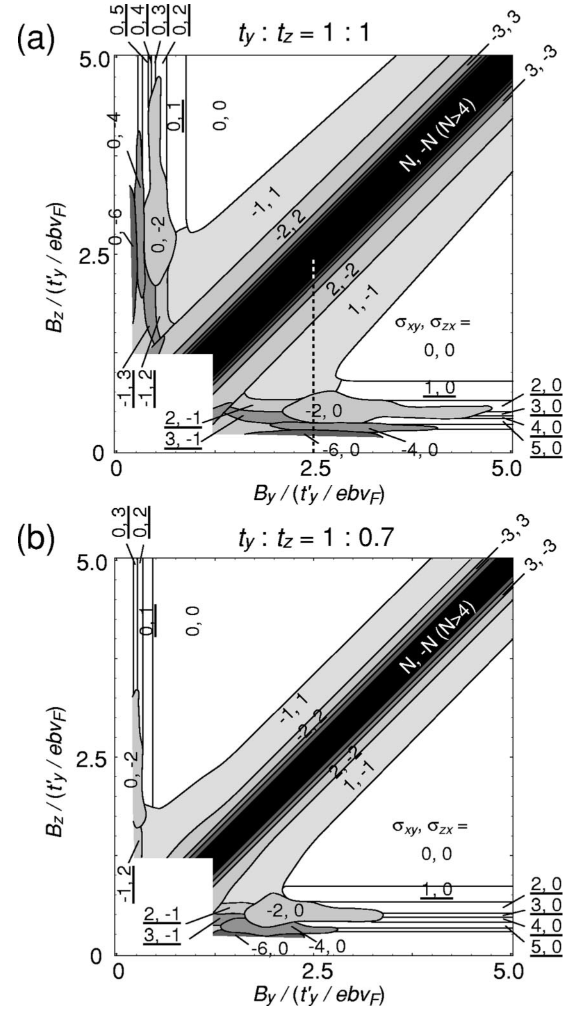

FIG. 2. The phase diagram for the FISDW in three dimensions at $T=0$ in the weak-coupling regime is shown against (B_y,B_z) for $t_z/t_y=1$ (a) or 0.7 (b) [i.e., $t_z'/t_y'=1$ (a) or 0.49 (b) in Eq. (4)]. The phases are labeled by the quantum Hall integers $(M,N)[=(\sigma_{xy},\sigma_{zx})$ in units of $(h/2e^2)]$, and those having $(q_y,q_z)\neq(\pi,\pi)$ are underlined. We assume $b=c$, $t_y/t_x=0.1$ and $\alpha=0.4$. The 3D-natured phases are shaded.

The integers (M,N) have an important physical meaning—the Hall conductivity. Following Yakovenko's formulation for two dimensions,[13] Sun and Maki[8] have predicted that the FISDW phase having (M,N) should have

Hall conductivities $(\sigma_{xy},\sigma_{zx})=(2e^2/h)(M,N)$ (2 is the spin factor). In our previous paper,[11] that demonstrated a realization of Hofstadter's butterfly in noninteracting 3D systems, we obtained quantum Hall integers residing on the fractal spectrum by making use of Streda's formula following Halperin, Kohmoto, and Wu,[12] where these integers are identified to be topological invariants assigned to each gap in the butterfly. If we apply this general argument to the FISDW problem treated here, the result coincides with Sun and Maki's. What is interesting about the FISDW states considered here ($t_y \sim t_z$) is that the wild variation of (M,N) with the magnetic field accompanies a wild variation in the quantum Hall conductivities.

The mathematical origin of the 3D phases can be traced back to the basic equations above (while we discuss the intuitive reason later). For $\theta \to 45°$, $G_b - G_c$ vanishes, and the argument of one of the Bessel functions, $J_{n_6}(z_6)$, diverges. Since $J_n(z)$ has the maximum at $z\sim n$, $\tilde{\Delta}(x)$ has a large Fourier component $e^{-in_6(G_b-G_c)x}$ with a nonzero n_6. If we assume other z's are small, I_{mn} has a maximum at $(m,n) = (n_6,-n_6)$, which corresponds to the $(N,-N)$ phases. Similarly, $(-2N,0)$ phases correspond to the divergence of $z_3 \propto 1/G_b$.

Now we come to the stability of the 3D phases. When we go from 3D systems over to 2D systems $[t_z(\text{or } t_y)\to 0]$, the 3D phases vanish and we are left with 2D phases with $N,0(0,N)$ that depend only on B_z (B_y), as seen from Fig. 2(b). These phases are known for $(\mathrm{TMTSF})_2X$, while the 3D phases are new. The nesting vector (q_y,q_z) is pinned to (π,π) in the $(N,-N)$ and $(-2N,0)$ phases, while in the 2D $(N,0)$ phases and some of 3D phases the nesting starts to deviate from (π,π) with N. We also note that the 3D phases do not require very large magnetic fields. In fact, when B_y or B_z becomes too large the 3D phases give way to 2D ones even when $t_y \simeq t_z$, as seen in Fig. 2(a). This is because a large in-plane component of $\boldsymbol{B}$ tends to confine the electron motion within each layer, so that the system becomes 2D-like.

3D FISDW phases with larger integers are less stable since I_{mn} (width of the energy gap) generally decreases with increasing m and n. Hence the FISDW should become unstable when the magnetic field is too close to $\theta=0$, 45°, or 90°, where the Hall integers diverge. In this region, some metallic phase may become stable, or some FISDW with (q_y,q_z) far from (π,π) may appear, while we have studied the range $0.9\pi \leqslant q_x,q_y \leqslant \pi$ here.

IV. ENERGY SPECTRUM

The second key result in this paper is the quasiparticle spectrum, which is plotted against B_z/B_y in Fig. 3(a). A structure reminiscent of Hofstader's butterfly are conspicuous around the Fermi energy. A closer examination reveals that the whole spectrum, consisting of various butterflies pieced together, is much more delicately constructed than a single butterfly. This is exactly because the optimized nesting vector [which jumps from one optimal (M,N) to another as $\boldsymbol{B}$ is varied] causes the spectrum to be pieced together in such a way that the Fermi energy always lies in the largest gap. For comparison, in Fig. 3(b) we display the energy spectrum when the optimization of the nesting vector is neglected with a fixed Δ. A zigzag trajectory of the position at which the largest gap occurs corresponds to the gap at $E=0$ in Fig. 3(a).

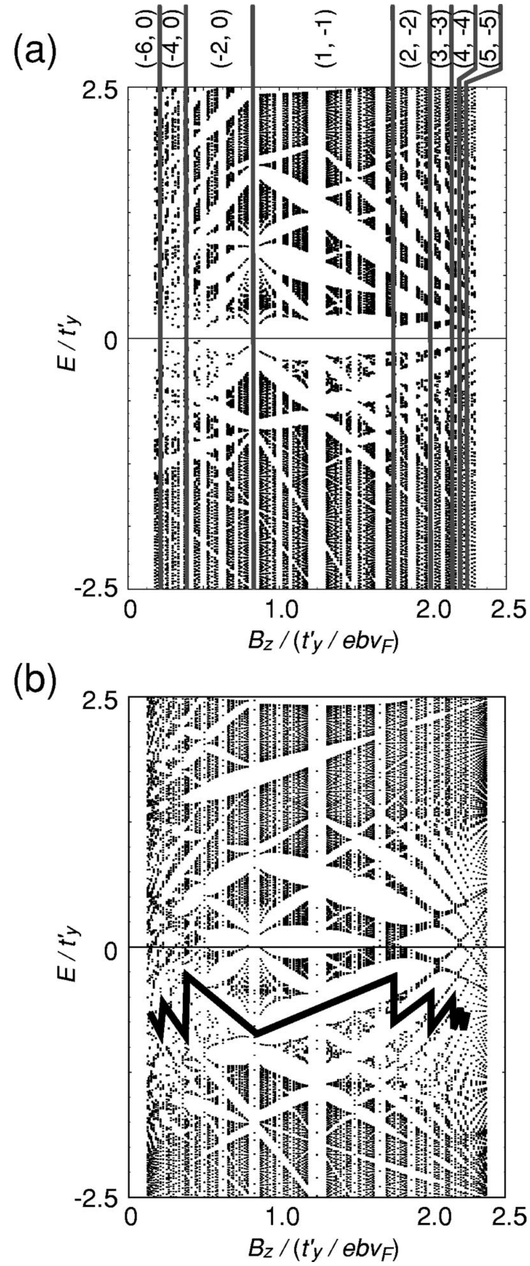

FIG. 3. (a) The quasiparticle energy spectrum against B_z for $t_z/t_y=1$ with B_y fixed to 2.5 (dashed line in Fig. 1). We assume a coupling constant $v_0D_0=0.34$ and the cut off energy $E_c=12.5t'_y$. Vertical lines indicate boundaries between different FISDW phases labeled by (M,N). (b) A similar spectrum when we do not optimize the nesting vector [i.e., $\boldsymbol{q}=(2k_F,\pi,\pi)$], with a fixed $\Delta(=0.5t'_y$ here), for comparison. The positions of the gaps having the largest I_{mn} are indicated by a solid line.

We can also trace back the mathematical reason why we have a butterfly. That is, the quasiparticle equation for the present system happens to coincide to that for the 3D butterfly in noninteracting systems previously studied,[11] in that the two periods G_b and G_c (arising from uniform $B_z$and B_y) compete with each other, where a difference is that the amplitude of the periodicity is here related to the order parameter Δ. So the spectrum plotted against B_z/B_y is in fact expected to have the same structure as Hofstadter's butterfly revealed in Ref. 11. An important distinction from the noninteracting case, however, is that the FISDW phase adjusts itself in such a way that the largest gap in the butterfly has the Fermi energy in it. So, while in the noninteracting case the butterfly structure is observed only around the bottom (or top) of the entire band, now we have the butterfly precisely around the Fermi level *by construction*, so the situation should be easier to realize experimentally.

V. DISCUSSIONS

Intuitive picture. To help understand the butterfly intuitively, we can look at the topology of the Fermi surface. If we first look at the case of the 3D butterfly in noninteracting systems, a typical Fermi surface around the band bottom consists of nearly parallel planes with a set of holes connecting them, as shown in Fig. 4(a). So we end up with, topologically, a coexistence of a bunch of pipes $\parallel y$ and another bunch $\parallel z$, and this induces a competition between the Landau quantizations due to B_y and B_z, which causes the 3D butterfly. If we go back to the present FISDW, we can see that the incompletely nested Fermi surface has a similar structure after the SDW gap formation, as typically shown in Fig. 4(b). There we display a warped Fermi surface in three dimensions, where the Fermi surface shifted by the nesting vector $\boldsymbol{q}$ is superimposed to show how they are interwoven. When the SDW gap opens in this incompletely nested Fermi surface in three dimensions, we have a *multiply connected Fermi surface* (i.e., a network of pipes) reminiscent of Fig. 4(a), as well as isolated pockets.

The situation sharply contrasts with the incompletely nested Fermi surface in two dimensions, where we end up with isolated pipes after the SDW formation. Thus the multiply connected Fermi surface explains how the butterflylike spectrum appears, although, to be more precise, there is a magnetic breakthrough across the pockets and the multiply connected Fermi surface. So we expect that the 3D butterfly tends to appear in systems having multiply connected Fermi surfaces.

Figure 4(b) also explains intuitively why SDW gaps are not formed for magnetic fields having $\theta \sim 0$, 45°, and 90°, since the semiclassical orbits on the multiply connected Fermi surface are open in this case, so that the SDW formation is not energetically favorable. Mathematically, the divergence of the arguments in Bessel functions mentioned above is related to the configuration of the Fermi "pipes."

Experimental possibilities. Experimentally, the best region to probe in the phase diagram (Fig. 2) to observe the 3D FISDW and the 3D butterfly should be where the 3D phase is observed for the entire tilting angle ($0<|\theta|<45°$) of the magnetic field with a fixed $|\boldsymbol{B}|$. This corresponds to a situation

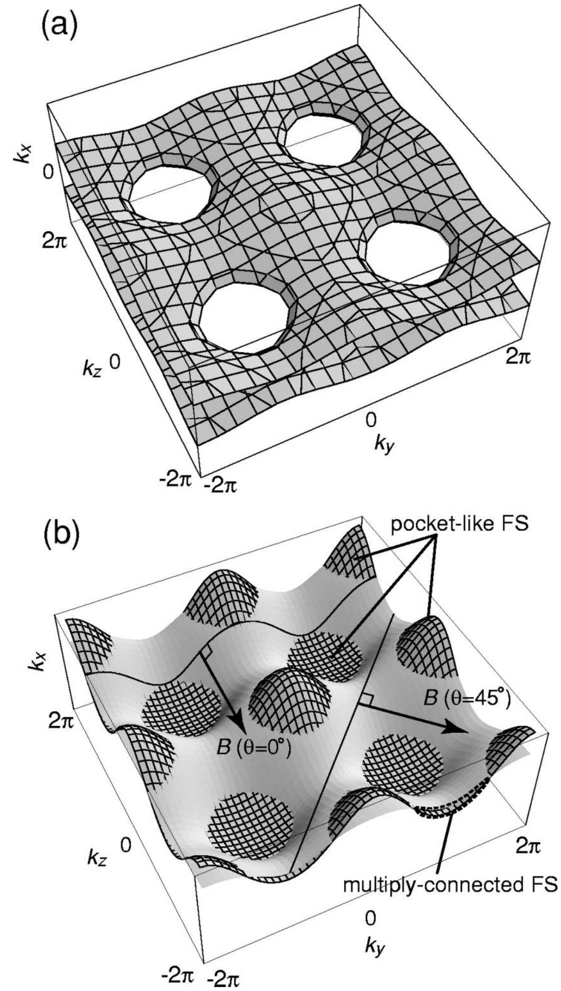

FIG. 4. (a) A typical Fermi surface for a noninteracting quasi-1D system with $t_x \gg t_y \sim t_z$ and $E_F \sim t_y, t_z$ from the band bottom. (b) A typical Fermi surface (mesh) superposed with the nested one (gray) translated by $\boldsymbol{q}$ for the 3D FISDW case. After the SDW gap opening, the Fermi surface consists of pockets and a multiply connected network of pipes. Solid lines exemplify open orbits for $\theta=0$ and 45°.

$$t'_y, t'_z \gtrsim eBbv_F. \tag{18}$$

Why this should be the criterion may be understood as follows. The basic equation is written in terms of $z_1 \ldots z_6$. As discussed above, the 3D butterfly is a result of a competition between the periods G_b and G_c. In other words, we need to have $z_3, \ldots, z_6 \gtrsim O(1)$, since $z_3, \ldots, z_6$ contributes to the Fourier component of G_b or G_c through $J_n(z)$. We can exclude z_1 and z_2 from our analysis, since they are always small when $(q_y, q_z) \simeq (\pi, \pi)$. So we end up with the criterion $t'_y, t'_z \gtrsim eBbv_F$ from the definition of $z_3, \ldots, z_6$ for $b \approx c$. We do not have to add a condition $t'_{yz}(\equiv 2\sqrt{t'_y t'_z}) \gtrsim eBbv_F$, since this condition is already included in the above one.

We can give a rough idea how we can realize the above condition. If we have a material with, say, $t'_y, t'_z \sim 10$ K [cf. $t'_y \sim 10$ K$\gg t'_z$ in $(TMTSF)_2X$] with values of v_F, b, and c similar to those in $(TMTSF)_2X$, then the butterfly and the peculiar quantum Hall effect should be observed for a moderate $B \lesssim 10$ T. The energy scale of the butterfly will be t'_y or t'_z, as seen in Fig. 3. To have a large FISDW gap energy scale, on the other hand, larger the $|B|$ the better, since for a small magnetic field (for which z's become large) I_{mn} has a spreaded distribution against m and n and the gaps become smaller.

ACKNOWLEDGMENTS

M.K. would like to acknowledge a Research Fellowship of the Japan Society for the Promotion of Science for Young Scientists for a financial support. He also wishes to thank Professor B.I. Halperin for his hospitality at Harvard University, where the manuscript was completed.

[1] L.P. Gor'kov and A.G. Lebed, J. Phys. (France) Lett. **45**, L433 (1984).
[2] D. Poilblanc, M. Héritier, G. Montambaux, and P. Lederer, J. Phys. C **19**, L321 (1986).
[3] K. Maki, Phys. Rev. B **33**, 4826 (1986).
[4] T. Ishiguro, K. Yamaji, and G. Saito *Organic Superconductors*, 2nd ed. (Springer, New York, 1998).
[5] A.G. Lebed, Pis'ma Zh. Eskp. Teor. Fiz. **43**, 174 (1986) [JETP Lett. **43**, 174 (1986)].
[6] G. Montambaux and P.B. Littlewood, Phys. Rev. Lett. **62**, 953 (1989).
[7] In principle, superconducting states are also possible, since magnetic fields, which generally suppress supreconductivity, can possibly, when extremely strong, help a reentrance of superconductivity in quasi-1D conductors as suggested by, e.g., N. Dupuis, G. Montambaux, and C.A.R. Sá de Melo, Phys. Rev. Lett. **70**, 2613 (1993). In our system, however, the required magnetic field for that would be much stronger than those for the FISDW.
[8] Y. Sun and K. Maki, Phys. Rev. B **49**, 15 356 (1994).
[9] Y. Hasegawa, Phys. Rev. B **51**, 4306 (1995).
[10] D.R. Hofstadter, Phys. Rev. B **14**, 2239 (1976).
[11] M. Koshino, H. Aoki, K. Kuroki, S. Kagoshima, and T. Osada, Phys. Rev. Lett. **86**, 1062 (2001).
[12] M. Kohmoto, B.I. Halperin, and Y. Wu, Phys. Rev. B **45**, 13 488 (1992).
[13] V.M. Yakovenko, Phys. Rev. B **43**, 11 353 (1991).